

# MEMS mirror-based 1×4 Core Selective Switch for 12-core fiber with low insertion-loss

Yuta Goto<sup>(1)</sup>, Ruben S Luis<sup>(1)</sup>, Yusuke Hirota<sup>(1)</sup>, Satoshi Shinada<sup>(1)</sup>, Sayaka Nagayama<sup>(2)</sup>, Asa Higashitani<sup>(2)</sup>, Tetsuya Kobayashi<sup>(2)</sup>, Ryohei Fukumoto<sup>(3)</sup>, and Hideaki Furukawa<sup>(1)</sup>

<sup>(1)</sup> National Institute of Information and Communications Technology (NICT), 4-2-1, Nukui-Kitamachi, Koganei, Tokyo, 184-8795, Japan, [y-goto@nict.go.jp](mailto:y-goto@nict.go.jp)

<sup>(2)</sup> OPTOQUEST Co., Ltd., 1335 Haraichi, Ageo, Saitama, 362-0021, Japan

<sup>(3)</sup> Optical Technologies R&D Center, Fujikura Ltd., 1440, Mutsuzaki, Sakura, Chiba, 285-8550, Japan

**Abstract** We demonstrate a novel MEMS mirror-based 1x4 core selective switch for 12-core multicore fiber. It achieves an insertion loss of less than 3.16 dB and negligible performance degradation on switching experiments.

## Introduction

Spatial division multiplexing (SDM) technologies have been actively researched, in order to support the rapid increase of internet traffic with a continuous growth of optical network capacity<sup>[1]</sup>. In these systems, the capacity is proportional to the number of spatial channels (SCs), which corresponds to the number of cores of multicore fiber (MCF) or the number of spatial modes of few-mode or multimode fibers. Recent demonstrations of high-capacity SDM transmission have shown over 10 Pb/s with more than 100 SCs<sup>[2],[3]</sup>. These systems have very high SC counts, which may be difficult to handle over meshed networks since the required switching resources increase by a factor proportional to the SC count<sup>[4],[5]</sup>.

A possible method to improve the resource requirements of SDM network switching is the use of a hierarchical SDM network architecture<sup>[6],[7]</sup>. In this case, the network has dedicated SDM and WDM network layers, using spatial channel cross-connect (SXC) and wavelength cross-connect (WXC) nodes, respectively. A 1 Pb/s network node based on this architecture was demonstrated, with as many as 22 SCs<sup>[8]</sup>. However, the network node used conventional single-core MEMS switches

supported by fan in/fan out (FIFO) devices to couple signals into and out of MCFs. Alternatively, the use of core selective switches (CSS) has been proposed<sup>[9]</sup>. Analogous to WSS, a CSS does not explicitly demultiplex the spatial channels, onto single-core devices. Instead, it is able to switch signals between cores of input and output MCFs. An LCOS-based CSS has been proposed for realizing a simple and compact CSS<sup>[9],[10]</sup>. However, the use of LCOS yields some disadvantages: the diffraction power loss, additional optical elements to maintain the polarization diversity, and slow operating speed. Using MEMS instead of LCOS for CSS without FIFO is very attractive because of its low loss. MEMS-based CSS have been demonstrated for 5-core fibers<sup>[11]</sup>.

Aiming to the high-throughput switching with many SCs, in this work, we demonstrate a novel 1x4 CSS for 12-core MCFs based on MEMS mirrors, as shown in Fig. 1. The core positions of 12-core fibers were aligned to accommodate a square grid of MEMS mirrors, in order to simplify its fabrication. There is scalability in the number of cores that can be accommodated without changing the configuration because our CSS has the extra mirrors. The CSS has an insertion loss (IL) of less than 3.2 dB and crosstalk (XT) below

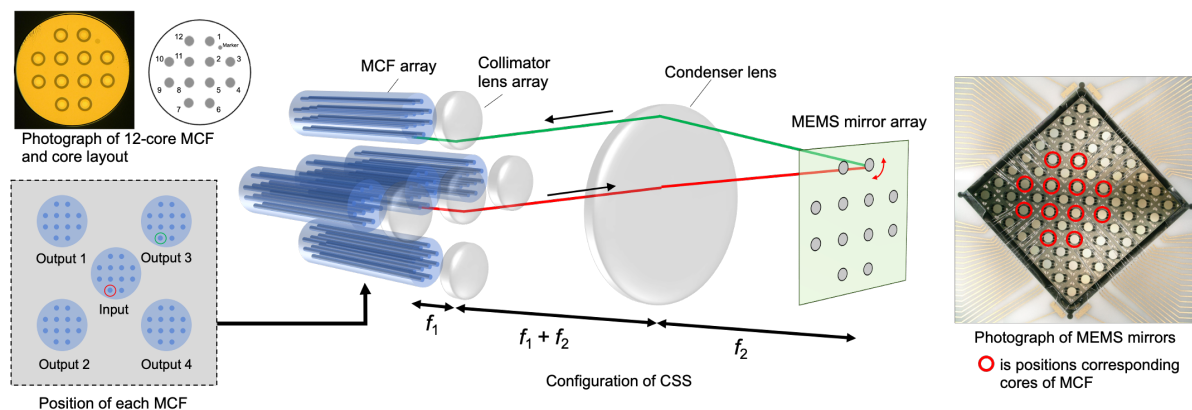


Fig. 1: MEMS mirror-based 1×4 CSS for 12-core fiber

-52 dB. It further achieved a switching time below 4 ms. We verify the switch properties and demonstrate its operation using 25 GBaud on-off keying (OOK) signals. The properties of the proposed switch render it potentially suitable for high capacity long distance transmission.

### MEMS mirror-based 1×4 CSS for 12-core fiber

The configuration of 12-core 1×4 CSS using MEMS mirrors and the positions of input and output MCFs array are shown in Fig. 1. The sectional image and core numbers of the 12-core MCFs and the picture of array of MEMS mirrors also shown in Fig. 1. The output MCFs 1 to 4 were arranged in a cross shape to surround the input MCF. Each collimator lens ( $f_1 = 1.8$  mm) was placed corresponding to the position of each MCF. The condenser lens ( $f_2 = 90.71$  mm) was placed at a distance of  $f_1 + f_2$  from the collimator lens so that these compose a 4f system. Note that the condenser lens was a combination lens consisting of two  $f = 150$  mm lenses. The MEMS mirror array was placed at distance of  $f_2$  from condenser lens, so the beam from each core was imaged on the MEMS mirror. As shown in the picture of the array of the MEMS mirrors in Fig.1, each mirror was circular and arranged in a grid pattern. The position of the mirrors was selected in order to correspond to the position of the cores of the 12-core MCF. In addition, the MCF with more cores can be accommodated because our CSS has the extra mirrors. The diameter and pitch of the mirrors were 0.8 mm and 2.4 mm, respectively. Parameters of 12-core MCF were the following: cladding diameter is 238  $\mu\text{m}$ , pitch of each core 48.0  $\mu\text{m}$ , and mode field diameter at 1550 nm is 11.7  $\mu\text{m}$ .

In the CSS, the beam from the input MCF was collimated and steered on the direction of the optical axis by the collimator lens. Therefore, the beam was obliquely incident on the condenser lens and focused on the MEMS mirror at the position corresponding to the core of the input MCF. By tilting the MEMS mirror in the desired direction, the reflected beam was steered and coupled with the desired output MCF via the collimating lens. Note that it was coupled to the

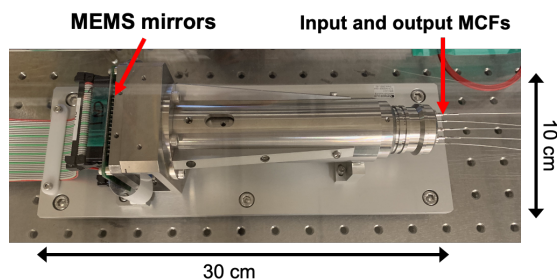


Fig. 2: Outward appearance of 12-core 1×4 CSS

only same core of the input MCF, considering the incidence angle on the output MCF. This switching principle is the same described in [9]-[11].

### Experimental results and discussion

Figure 2 shows the outward appearance of 12-core 1×4 CSS. The desired output MCF can be set via software. Unfortunately, some mirrors are inoperable due to contamination with fine dust in the manufacturing process of the MEMS. The position of the inoperable mirror corresponded to that of cores 4 and 6 of the MCFs. This problem can be solved in the future.

First, we measured the IL and XTs in each output MCF for evaluating the performance of the free-space optics in our CSS. In the experiment, FIFOs were used for only connecting between the single core fibers of the measurement instruments and the CSS, not for switching. In the measurement of IL and XT, light from an amplified spontaneous emission (ASE) source was split to four branches by a 1×4 coupler, each branch was connected to output MCFs. At the time, the beam propagating from the desired output MCF to input MCF, is IL and lights from other MCF are XTs. For distinguishing the IL and XTs, the ASE were connected individually. In the case of measuring output MCF 1, the IL can be measured by connecting the ASE to only output MCF 1, and total (in the worst case) XT can be measured by connecting the ASE to output MCF 2, 3 and 4 simultaneously. The measured IL and XTs on the C-band (1530 nm to 1565 nm) is shown in Fig. 3. From Fig. 3, it can be seen that IL and XT are quite small. In fact, the range of the IL was 1.37 dB to 3.57 dB. In addition, since the FIFOs has the loss of 0.18 dB to 0.41dB, we can say that the actual IL was 1.16dB to 3.16 dB. Moreover, the polarization dependent loss of our CSS was 0.01 dB to 0.05 dB at 1550 nm.

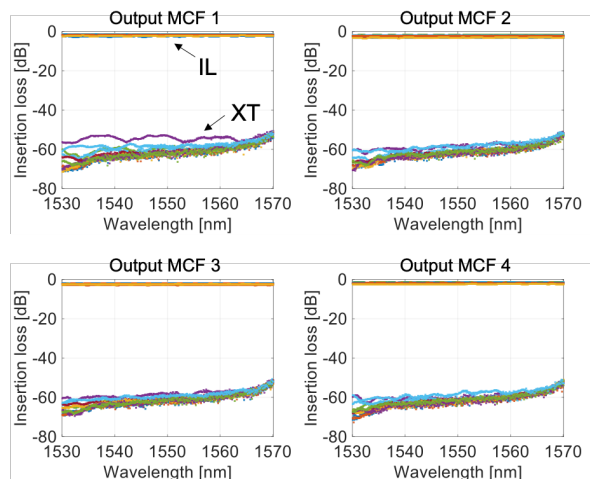


Fig. 3: IL and XTs of MEMS based CSS

Next, the switching speed of our CSS was evaluated. In the experiment, the CSS was switched from output MCF 2 to output MCF 1 while the CW light was incident on the input MCF, at that time, the time variation of the optical power on the output MCF 1 was acquired with a 350 MHz oscilloscope. Figure 4 shows the optical power obtained with the oscilloscope when switching CSS. In Fig. 4, although there are fluctuations, it can be seen that the optical output rises due to switching by MEMS mirror. The rise time and the optical power was approximately 3.25 msec. Considering that the operating speed of the commercially available LCOS is generally few hundreds of msec<sup>[12]</sup>, MEMS mirror-based CSS has an advantage in switching time.

Finally, we evaluated the quality on switching operation for 25 GBaud OOK optical signals using our CSS. Figure 5 shows the experimental

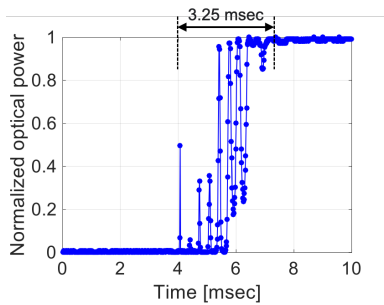


Fig. 4: Optical power when switching CSS

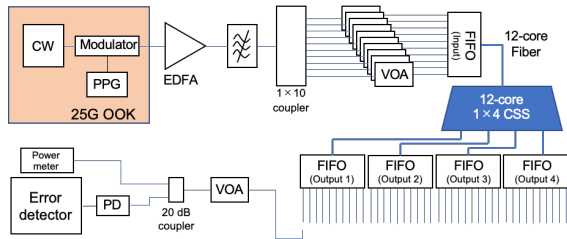


Fig. 5: Experimental setup for 25G OOK switching

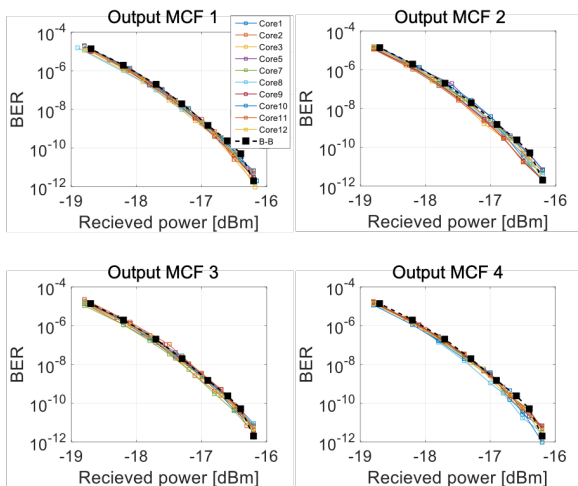


Fig. 6: BER vs received power

setup. The OOK signals generated by the pulse pattern generator (PPG) and the intensity modulator was split to ten branches and connected to CSS by the input FIFO. Then, the BER of all ports and all cores was measured by the error detector. Figure 6 shows the BER versus received power characteristic. The degradation in the penalty of each output MCF was not observed compared to the back-to-back measurement by directly connecting the input and each output FIFO.

## Conclusions

We demonstrated MEMS mirror-based 1x4 CSS for 12-core fibers. The IL of less than -3.16 dB, the XTs below -52 dB and the switching speed of approximately 3.25 msec has been achieved on our CSS. In addition, we confirmed that the negligible performance degradation on switching experiment with 25 GBaud OOK optical signals was achieved. This CSS can contribute long span transmission and multi-node hopping of high capacity optical signals. In the future, we will demonstrate the CSS with more SCs for the high-throughput switching.

## References

- [1] D. Richardson *et al.*, "Space-division multiplexing in optical fibres", *Nature Photon*, vol.7, 354–362, 2013.
- [2] D. Soma *et al.*, "10.16 Peta-bit/s Dense SDM/WDM transmission over Low-DMD 6-Mode 19-Core Fibre Across C+L Band," *2017 European Conference on Optical Communication (ECOC)*, pp. 1-3, 2017.
- [3] G. Rademacher *et al.*, "10.66 Peta-Bit/s Transmission over a 38-Core-Three-Mode Fiber," *2020 Optical Fiber Communications Conference and Exhibition (OFC)*, pp. 1-3, 2020.
- [4] D. M. Marom *et al.*, "Survey of photonic switching architectures and technologies in support of spatially and spectrally flexible optical networking [Invited]," *J. Opt. Commun. Netw.*, vol. 9, no. 1, pp. 1-26, 2017.
- [5] R. Hashimoto *et al.*, "First demonstration of subsystem-modular optical cross-connect using single-module 6 × 6 wavelength-selective switch," *J. Lightw. Technol.*, vol. 36, no. 7, pp. 1435-1442, 2018.
- [6] M. Jinno, "Spatial channel network (SCN): Opportunities and challenges of introducing spatial bypass toward the massive SDM era [invited]," *J. of Optical Comm. and Networking*, vol. 11, no. 3, pp. 1-14, 2019.
- [7] M. Jinno *et al.*, "Feasibility demonstration of spatial channel networking using SDM/WDM hierarchical approach for Peta-b/s optical transport", *J. of Lightw. Technology*, vol. 38, no. 9, pp. 2577-2586, 2020.
- [8] R. S. Luis *et al.*, "Demonstration of a 1 PB/S spatial channel network node," *45th European Conference on Optical Communication (ECOC 2019)*, pp. 1-4, 2019.
- [9] M. Jinno *et al.*, "Architecture and feasibility demonstration of core selective switch (CSS) for spatial channel network (SCN)", *OECC/PSC*, pp. WA2-3, 2019.
- [10] M. Jinno *et al.*, "Five-Core 1x6 Core Selective Switch

and Its Application to Spatial Channel Networking," *2020 Optical Fiber Communications Conference and Exhibition (OFC)*, pp. 1-3, 2020.

[11] M. Jinno *et al.*, " Ultra-Wideband and Low-Loss Core Selective Switch Employing Two-Dimensionally Arranged MEMS Mirrors," *2021 Optical Fiber Communications Conference and Exhibition (OFC)*, W1A.3, 2021.

[12] <https://www.santec.com/en/about/coretechnology/lc/>